CAN ANISOTROPIC IMAGES BE UPSAMPLED?

Mads F. Hansen, Thomas H. Mosbech, Hildur Ólafsdóttir, Michael S. Hansen and Rasmus Larsen
DTU Informatics, Technical University of Denmark, Richard Petersens Plads, Kgs. Lyngby, Denmark

Keywords: Image reconstruction, Image registration, Riemannian elasticity, Super resolution penalization prior.

Abstract: This paper presents a novel method for upsampling anisotropic medical gray-scale images. The resolution is increased by fitting an image function, modeled by cubic B-splines, to the slices. The method simulates the observed slices with an image function and iteratively updates the function by comparing the simulated slices with observed slices. The approach handles partial voluming by modeling the thickness of the slices. The formulation is ill-posed, and thus a prior needs to be included. Correspondences between adjacent slices are established using a symmetric registration method with a free-form deformation model. The correspondences are then converted into a prior that penalizes gradients along lines of correspondence. Tests on the Shepp-Logan phantom show promising results, and the approach performs better than methods such as cubic interpolation and one-way registration-based interpolation.

1 INTRODUCTION

Image interpolation plays an important role in many medical image analysis applications by closing the gap between the true continuous nature of an image and the practical discrete representation of an image. Uniform tensor splines (UTS), e.g. tricubic interpolation, is the method of choice for most applications due to the regular sampling of discrete images. A potential problem with this approach is the inherent assumption of a smooth transition between neighboring voxels.

The idea of *registration-based interpolation* was introduced as a solution to the problem (Penney et al., 2004). Here, correspondences between neighboring slices are determined by one-way registrations in 2D. The interpolation is then performed along these lines of correspondence to achieve a smooth transition, rather than using the usual lateral neighborhood.

The method was extended by utilizing both a forward and backward registration – a weighted sum of two non-symmetric displacement fields – for the interpolation (Frakes et al., 2008).

Recently, (Ólafsdóttir et al., 2010) proposed a method to improve the method even further. The paper presents an interpolation based on weighting both intensity and deformation by the inter-slice distance of the interpolation point. The method combines both a forward and backward interpolation into a less time-consuming algorithm in comparison to (Penney et al., 2004) by using an approximation to the inverse deformation, while still reporting sufficiently accurate results.

The quality of registration-based interpolation is highly dependent on the quality of the correspondences obtained. This can be somewhat questionable as there may not exist a one-to-one mapping between adjacent slices. That is, structures may disappear between two slices, and in these situations one must rely on the *nice* behavior of the chosen registration scheme. Another previously untouched problem in registration-based interpolation is the partial volume effect; image artifacts occurring as part of the image digitalization, where images are formed by slices of thick volumetric blocks rather than infinitely thin 2D planes.

As an alternative to the common registration-based interpolation we propose fitting a *parametric function* to the thick slices, accounting for the partial volume effect by incorporating the thickness of a slice. Furthermore, we use symmetric registration between adjacent slices to form a prior to stabilize the ill-posed problem.

As the idea behind the method is to identify the underlying image rather than interpolating the thick slice voxels, we say the method *upsamples* the anisotropic image under reasonable constraints.

F. Hansen M., H. Mosbech T., Ólafsdóttir H., S. Hansen M. and Larsen R. (2010).
CAN ANISOTROPIC IMAGES BE UPSAMPLED?.
In *Proceedings of the International Conference on Computer Vision Theory and Applications*, pages 76-81
DOI: 10.5220/0002846500760081
Copyright © SciTePress

2 METHODS

The goal of our method is to obtain a better approximation of the true 3D image R given a slice-based representation defined by the set of K slices $\{S^1, S^2, \ldots, S^K\}$. Here, a slice is a 2D planar view of a 3D image integrated over a given thickness. That is, the expected value of the (i,j)th voxel of the kth slice image S^k_{ij} is given by

$$E[S^k_{ij}|R] = \int_{V_{ij}} R(\boldsymbol{x})dv, \tag{1}$$

where V_{ij} is the volume element covered by the (i,j)th voxel. When this volume contains a mixture of multiple tissue values, the partial volume effect occurs. This is particularly evident for thicker slices – images with more anisotropic voxels.

2.1 Upsampling Strategy

Our strategy for upsampling is to iteratively update an approximation $\tilde{R}$ of the true image R by comparing the current approximation with the observed slices. To do this we formulate the quality of match as

$$\mathcal{M}[\tilde{R}, \{S^k\}_{k=1\ldots K}] = \sum_{k=1}^{K}\sum_{i=1}^{M}\sum_{j=1}^{N} m(E[S^k_{ij}|\hat{R}], S^k_{ij}), \tag{2}$$

where $m(\cdot)$ is a measure of similarity between voxels in the observed and simulated slices. Here, we use cubic B-splines as the parametric representation of $\tilde{R}$

$$\tilde{R}(\boldsymbol{x}, \boldsymbol{p}) = \langle \boldsymbol{b}(x_3) \otimes \boldsymbol{b}(x_2) \otimes \boldsymbol{b}(x_1), \boldsymbol{p} \rangle, \tag{3}$$

where $\boldsymbol{p}$ are the image parameters, and $\boldsymbol{b}$ are the B-splines. The most suitable measure of similarity is dependent on the underlying noise model of the data. For intensities in magnetic resonance images (MRI) with a high signal-to-noise ratio, the noise is approximately Gaussian (Gudbjartsson and Patz, 1995). Thus, assuming i.i.d. the squared difference in intensities optimally defines the similarity between observation and simulation

$$m(E[S^k_{ij}|\hat{R}], S^k_{ij}) = (E[S^k_{ij}|\hat{R}] - S^k_{ij})^2. \tag{4}$$

Given this parametric representation of $\tilde{R}$, it is possible to obtain a continuous representation of R by minimizing (2) with respect to the parameters. This can reduce the partial volume effect. Unfortunately, the minimization is unlikely to produce a better approximation to the true R as the problem is ill-posed. Thus, more information needs to be added in order to solve the problem properly. We seek to handle this

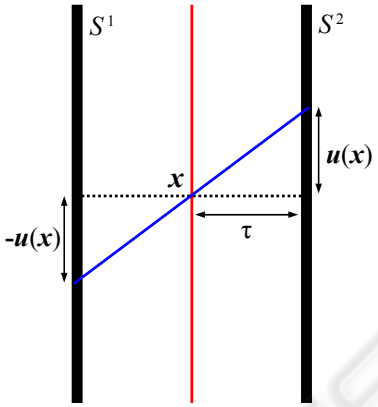

Figure 1: Illustration of slice registration setup and direction of penalization vector field.

this by including a prior $\mathcal{S}$ in the cost function. That is, a new approximation $\tilde{R}$ is obtained by solving

$$\min_{\tilde{R}} \mathcal{M}[\tilde{R}, \{S^k\}_{k=1\ldots K}] + \beta \mathcal{S}_{\boldsymbol{v}}[\tilde{R}], \tag{5}$$

where the coefficient β governs the effect of the prior.

In this work, we specifically consider a penalty term that penalizes high image gradients in certain directions. We write the prior as the inner product between the gradient image and a vector field $\boldsymbol{v}$, i.e.

$$\mathcal{S}_{\boldsymbol{v}}[\tilde{R}] = \int_{\Omega} \langle \nabla \tilde{R}(\boldsymbol{x}), \boldsymbol{v}(\boldsymbol{x}) \rangle^2 d\boldsymbol{x}, \tag{6}$$

That is, $\boldsymbol{v}$ determines the direction and magnitude of the penalty – resulting in less regularization where the two are approximately orthogonal and/or of low magnitude. We call $\boldsymbol{v}$ the *penalization vector field*. The following section presents a procedure for constructing this vector field.

2.2 Constructing a Penalization Vector Field

Inspired by (Penney et al., 2004; Frakes et al., 2008; Ólafsdóttir et al., 2010) we obtain the penalization vector field by non-rigid registration of neighboring slices. We apply a symmetric registration between slices, assuming that the point $\boldsymbol{\phi}_1(\boldsymbol{x}) = \boldsymbol{x} - \boldsymbol{u}(\boldsymbol{x})$ in slice S^1 corresponds to the point $\boldsymbol{\phi}_2(\boldsymbol{x}) = \boldsymbol{x} + \boldsymbol{u}(\boldsymbol{x})$ in slice S^2. The concept is illustrated in Figure 1. The penalization vector field is then composed by a half slice thickness τ, the displacement $\boldsymbol{u}$ and a scale factor γ

$$\boldsymbol{v}(\boldsymbol{x}) = \gamma(\boldsymbol{x}) \frac{[\tau,\ \boldsymbol{u}(\boldsymbol{x})]^{\mathrm{T}}}{\| [\tau,\ \boldsymbol{u}(\boldsymbol{x})]^{\mathrm{T}} \|}. \tag{7}$$

The squared difference similarity measure drives the registration as we assume that intensities in adjacent slices are directly comparable, and that the noise is i.i.d., i.e.

$$\mathcal{D}[S^1, S^2; \boldsymbol{u}] = \int_\Omega \left(S^2 \circ \boldsymbol{\phi}_2(\boldsymbol{x}) - S^1 \circ \boldsymbol{\phi}_1(\boldsymbol{x})\right)^2 d\boldsymbol{x}, \quad (8)$$

with $S^i(\boldsymbol{\phi}_i(\boldsymbol{x})) = S^i \circ \boldsymbol{\phi}_i(\boldsymbol{x})$.

The free-form deformation model (Rueckert et al., 1999) is used to model the deformation $\boldsymbol{u}$ in order to reduce the dimensionality of the problem. Hence,

$$\boldsymbol{u}(\boldsymbol{x}; \boldsymbol{w}) = \langle \boldsymbol{b}(x_2) \otimes \boldsymbol{b}(x_1), \boldsymbol{w} \rangle, \quad (9)$$

where $\boldsymbol{w}$ are the deformation parameters, and $\boldsymbol{b}$ are the B-splines.

To ensure a homeomorphic deformation we adapt the Riemannian elasticity energy (Pennec et al., 2005) in the registration process. The elasticity energy of a deformation field $\boldsymbol{\phi}$ is given by

$$\mathcal{S}_{rie}(\boldsymbol{\phi}) = \int_\Omega \mu \, \mathrm{tr}(\boldsymbol{E}_0(\boldsymbol{x})^2) + \frac{\lambda}{2} \mathrm{tr}(\boldsymbol{E}_0(\boldsymbol{x}))^2 d\boldsymbol{x} \quad (10)$$

where $\boldsymbol{E}_0 = \frac{1}{2} \log((\boldsymbol{I} + \nabla\boldsymbol{\phi})^T (\boldsymbol{I} + \nabla\boldsymbol{\phi}))$ is the Hencky strain tensor.

Thus, correspondences between adjacent slices are identified by solving

$$\min_{\boldsymbol{w}} \mathcal{D}[S^1, S^2; \boldsymbol{u}] + \alpha(\mathcal{S}_{rie}(\boldsymbol{\phi}_1) + \mathcal{S}_{rie}(\boldsymbol{\phi}_2)), \quad (11)$$

where α determines the amount of regularization introduced by the elasticity term.

Homogeneous areas in the image (e.g. background) contain no information to guide the registration. Therefore, one should be cautious when putting great confidence in the local correspondences estimated here. To address this issue we introduce an information score e for each registration point. This is included by means of the scale factor γ of the penalization vector field (7).

We base e on the edge information available in the slice around each position, as edges *within* slices are valuable in the registration. For a point $\boldsymbol{x}$ we filter around the position in the two neighboring image slices $\boldsymbol{\phi}_1(\boldsymbol{x})$ and $\boldsymbol{\phi}_2(\boldsymbol{x})$ with the first order derivative of a 1D Gaussian kernel (Canny, 1986)

$$G'_\sigma(x) \frac{\partial G_\sigma(x)}{\partial x} = \frac{-x}{\sigma} \frac{1}{\sigma\sqrt{2\pi}} \exp - \frac{x^2}{2\sigma^2}. \quad (12)$$

The kernel covers n pixels on each side of the pixel and has a standard deviation of $\sigma = n/3$.

The score is then computed as the absolute value of the sum of the two

$$e(\boldsymbol{x}) = \left| G'_\sigma * \left(S^1 \circ \boldsymbol{\phi}_1(\boldsymbol{x})\right) + G'_\sigma * \left(S^2 \circ \boldsymbol{\phi}_2(\boldsymbol{x})\right) \right|. \quad (13)$$

This means that both slices must contain edge information around the matching point in order for the correspondence to be regarded as strong.

The scale factor is then computed as the score divided by a parameter ε plus the similarity measure of (8)

$$\gamma(\boldsymbol{x}) = \frac{e(\boldsymbol{x})}{\varepsilon + \left(S^2 \circ \boldsymbol{\phi}_2(\boldsymbol{x}) - S^1 \circ \boldsymbol{\phi}_1(\boldsymbol{x})\right)^2}. \quad (14)$$

where the value of ε is related to the intensity level of the image. As mentioned earlier, the penalization vector field is then constructed by multiplying the correspondence directions from the registration by these scale factors.

3 EXPERIMENTS

In this section we present a study in 2D comparing our proposed upsampling approach using the prior of the penalization vector field (UPWP) against the standard cubic interpolation (CI) (Keys, 1981) and the one-way registration-based interpolation (RBI) (Penney et al., 2004). For reference we also include a reconstruction performed using our method without the prior (UPNP).

From a 250×250 isotropic-sampled Shepp-Logan phantom (Shepp and Logan, 1974) we create a downsampled anisotropic image by averaging every five columns together. Figures 2(a,b) show the isotropic and anisotropic phantom. That is, the columns act as the thick slices in the context described in the previous section. Figure 2(c) displays the registration-based line correspondences superimposed on the anisotropic phantom. For the registration the knot spacing of the B-splines was four pixels and the regularization weight was 10^{-2}. A penalization vector field was extracted from the registration. The columns were filtered using the derivative of a 1D Gaussian kernel with standard deviation $\frac{5}{3}$. The resulting field is displayed in Figure 2(d).

Four reconstructions were obtained from the anisotropic-sampled phantom using CI, RBI and our UPNP and UPWP without and with the penalization vector field shown in Figure 2(d). Figure 3 contains these reconstructions. For quantitative comparison we computed the mean squared error (MSE) between pixel values in the isotropic-generated phantom and the reconstructions. Table 1 lists the results. From Figure 3 and Table 1 we acknowledge that UPWP

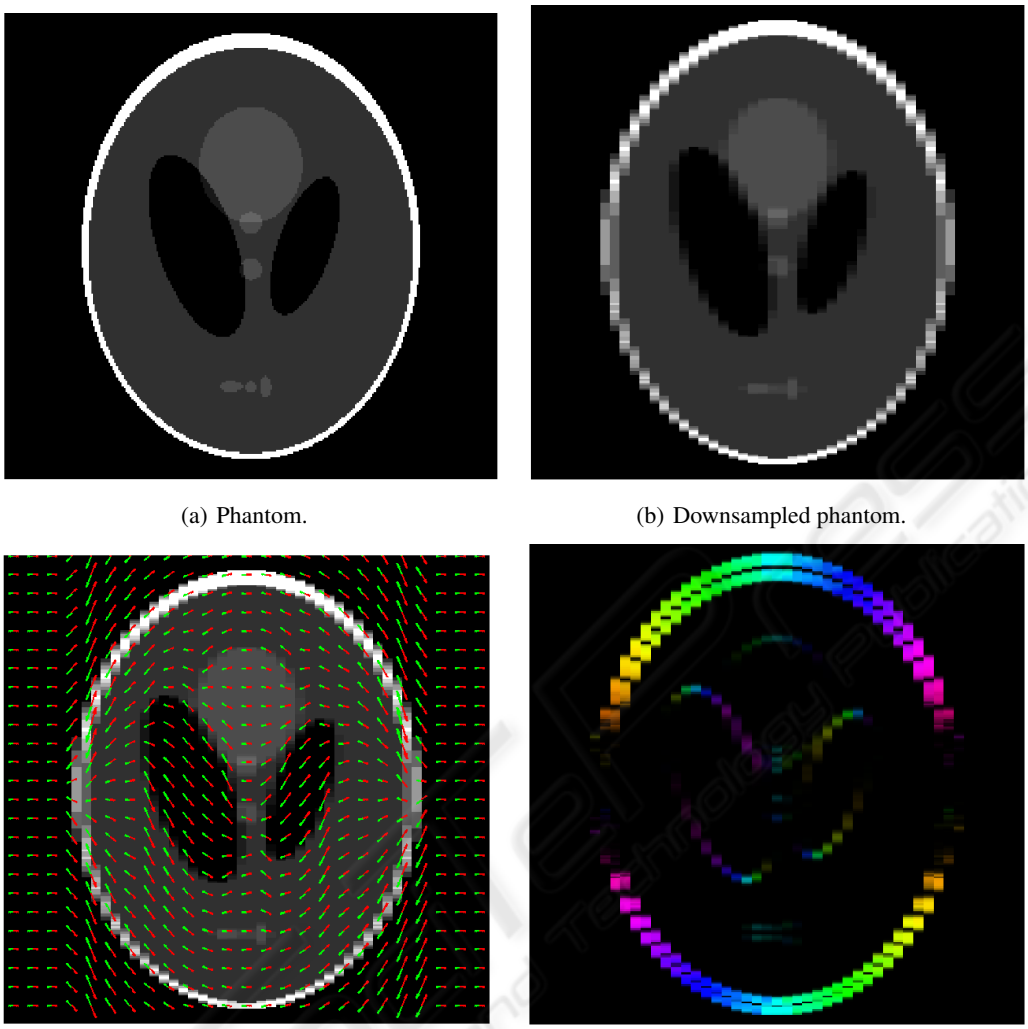

(a) Phantom.

(b) Downsampled phantom.

(c) Downsampled phantom with correspondences from the registration.

(d) Penalization vector field.

(e) Color-map for penalization vector field field. The color shows the direction and the brightness shows the magnitude.

Figure 2: Visualization of phantom data, symmetric registration and the penalization vector field.

provides the most visually pleasing result as well as the lowest MSE. Finally, we see from Figure 3(b) that the RBI approach provides visually nice interpolation in areas with good registration, and unsatisfactory interpolation in areas lacking correspondences – areas where structures runs approximately parallel to the slices. This problem and the method's ability to recover from partial volume effects of the upsampling approach explain the lower MSE of our UPWP.

(a) Cubic interpolation.

(b) One-way registration (Penney et al., 2004).

(c) Upsampling without prior.

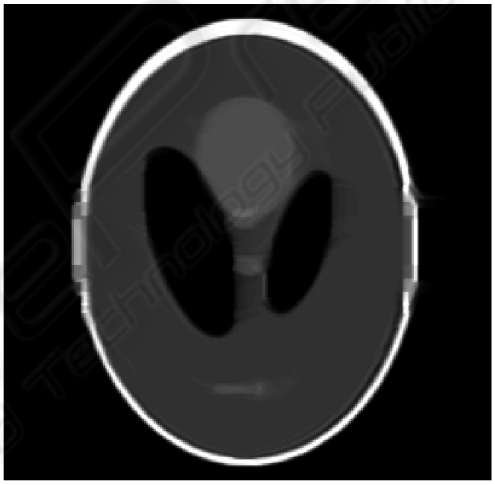

(d) Upsampling with prior.

Figure 3: Reconstructions.

Table 1: Mean squared error between reconstructions and isotropic phantom for the four reconstruction methods.

	CI	RBI	UPNP	UPWP
MSE	0.0143	0.0073	0.0080	0.0045

4 CONCLUSIONS

This paper presented a novel approach for improving the resolution of anisotropic medical images. The method relies on a prior constructed upon registrations of neighboring slices. As such, the quality of the prior is undoubtedly dependent on the quality of the registrations. However, unlike the registration-based interpolation method, it is possible to limit the effect of mis-registrations by reducing the length of the penalization vector field in areas with little information or poor fit. The preliminary tests presented in the paper showed promising results, motivating further investigation and validation.

REFERENCES

Canny, J. (1986). A computational approach to edge detection. *IEEE Transactions Pattern Analysis and Machine Intelligence*, 8(6):679–698.

Frakes, D., Dasi, L., Pekkan, K., Kitajima, H., Sundareswaran, K., Yoganathan, A., and Smith, M. (2008). A New Method for Registration-based Medical Image Interpolation. *IEEE Transactions on Medical Imaging*, 27(3):370–377.

Gudbjartsson, H. and Patz, S. (1995). The rician distribution

of noisy mri data. *Magnetic Resonance in Medicine*, 34(6):910–914.

Keys, R. G. (1981). Cubic Convolution Interpolation for Digital Image Processing. *IEEE Transactions on Acoustics Speech and Signal Processing*, 29(6):1153–1160.

Ólafsdóttir, H., Pedersen, H., Hansen, M. S., Lyksborg, M., Darkner, S., and Larsen, R. (2010). Registration-based Interpolation Applied to Cardiac MR. *Proceedings of SPIE Medical Imaging 2010: Image Processing*.

Pennec, X., Stefanescu, R., Arsigny, V., Fillard, P., and Ayache, N. (2005). Riemannian Elasticity: A Statistical Regularization Framework for Non-linear Registration. *Proceedings of the 8th International Conference on Medical Image Computing and Computer-Assisted Intervention (LNCS)*, 3750:943–950.

Penney, G., Schnabel, J., Rueckert, D., Viergever, M., and Niessen, W. (2004). Registration-based Interpolation. *IEEE Transactions on Medical Imaging*, 21(7):922–926.

Rueckert, D., Sonoda, L. I., Hayes, C., Hill, D. L. G., Leach, M. O., and Hawkes, D. J. (1999). Nonrigid Registration using Free-Form Deformations: Application to Breast MR Images. *IEEE Transactions on Medical Imaging*, 18(8):712–21.

Shepp, L. A. and Logan, B. F. (1974). The Fourier reconstruction of a head section. *IEEE Transactions on Nuclear Science*, 21(3):21–43.

SciTePress
Science and Technology Publications